Journal of Applied Physics

RESEARCH ARTICLE | APRIL 27 2017

# Quantitative analysis of domain textures in ferroelectric ceramics from single high-energy synchrotron X-ray diffraction images

Zhiyang Wang; John E. Daniels



*J. Appl. Phys.* 121, 164102 (2017)
https://doi.org/10.1063/1.4982674

# Quantitative analysis of domain textures in ferroelectric ceramics from single high-energy synchrotron X-ray diffraction images

Zhiyang Wang[1,2,a)] and John E. Daniels[1]
[1]*School of Materials Science and Engineering, UNSW Australia, Sydney, New South Wales 2052, Australia*
[2]*Australian Synchrotron, 800 Blackburn Road, Clayton, Victoria 3168, Australia*

(Received 30 November 2016; accepted 15 April 2017; published online 27 April 2017)

In this study, the possibility of determining the orientation distribution function (ODF) and quantifying the domain textures of polycrystalline ferroelectrics based on single high-energy X-ray diffraction images using a Rietveld refinement method is assessed. A spherical harmonics texture model is incorporated in the approach to determine the ODFs for phase constituents in poled lead-free ferroelectric ceramics $(1-x)(Bi_{0.5}Na_{0.5})TiO_3 - xBaTiO_3$ with $x = 0.0625$ and 0.075 from both single high-energy synchrotron diffraction images and full rotation diffraction data collected with the samples rotated perpendicular to the poling axis. A quantitative comparison is made between the complete pole figures and pole density profiles obtained from the ODFs extracted from the different diffraction data. The results show that a good approximation to the domain textures of fiber-type in poled ceramics as determined from the full rotation data can be obtained from single diffraction images, with the dominant pole densities within a maximum difference of ~0.15 multiples of a random distribution. It thus demonstrates that single high-energy X-ray diffraction images are suitable for the quantification of domain texture in ferroelectric ceramics. The analysis validates the applicability of high-energy synchrotron X-day diffraction to observe the texture evolution *in situ* in ferroelectric ceramics under fast or continuous loading conditions. *Published by AIP Publishing*. [http://dx.doi.org/10.1063/1.4982674]

## I. INTRODUCTION

Piezoelectric ceramics are extensively used for a variety of technological applications in electromechanical devices such as sensors and actuators. In these materials, non-180° ferroelectric/ferroelastic domains exist that couple both a spontaneous electrical polarization and a spontaneous strain, i.e., the changes in the electrical polarization will influence the strain state of materials while changes in stress can reorient the electrical polarization. Under an externally applied mechanical stress or electric field, these domains tend to reorient such that the ferroic order parameter orients with respect to the external field direction. Specifically, the applied electric field or tensile stress will preferentially align the spontaneous polarization of domains to the applied electric field or uniaxial tensile stress direction, while an applied uniaxial compressive stress will tend to align the spontaneous polarization of domains perpendicular to the compressive stress axis. This field-induced non-180° domain switching increases the volume fraction of non-180° ferroelectric/ferroelastic domains aligned with the applied electric field, resulting in a domain texture in the polycrystalline material.[1] The domain texture is an important characteristic of the microstructure of polycrystalline ferroelectric thin films and ceramics, affecting many of their functionalities.[2,3] In particular, the evolution of domain textures in ferroelectric ceramics resulting from the non-180° domain switching process determines the extrinsic component of their electromechanical properties. Quantitative characterization of domain textures in polycrystalline ferroelectrics both *in situ* and *ex situ* is therefore requisite for understanding the underlying microstructural origin of their electromechanical responses.

Diffraction techniques based on X-ray/neutron and electron probes are commonly applied to measure the texture in polycrystalline materials. Compared with constant-wavelength neutron diffraction and electron backscattered diffraction (EBSD) methods, high-energy synchrotron X-ray diffraction ($E > \sim 60$ keV) in combination with large area detectors enables the probing of a large range of crystalline orientations in individual exposures, offering the advantages of fast texture measurements.[4–7] This capability of fast texture characterization is increasingly required for spatially resolved texture mapping and to follow the texture evolution in polycrystalline materials under situations, where the texture changes occur rapidly, such as during the polarization reversal of ferroelectric ceramics.[8]

For quantitative texture analysis with high-energy synchrotron diffraction, the orientation distribution function (ODF) of textured materials is conventionally determined from pole figure measurements based on the collected Debye–Scherrer diffraction images at various sample orientations.[9] In some cases of high crystal symmetry (cubic and hexagonal) materials, it has been demonstrated that quantitative texture information can be extracted from a single high-energy synchrotron diffraction image with a good approximation to the full ODF obtained using full-pattern Rietveld refinement approach.[6,7,10] For a randomly oriented piezoelectric ceramic material, a field-induced non-180° ferroelectric/ferroelastic fiber domain texture is expected due to the vector field nature of an applied electric field. Some attempts have also been made to quantify the textures in ferroelectric

a)Author to whom correspondence should be addressed. Electronic mail: zhiyang.wang@synchrotron.org.au. Tel.: +61 03 85405397.

ceramics based on single high-energy diffraction images using this Rietveld approach assuming fiber sample symmetry.[11–14] However, whether a complete description of the ferroelectric domain textures in ceramics can be obtained from single high-energy synchrotron diffraction images is yet to be verified.

In the present work, the domain textures due to electrical poling of $(1-x)(Bi_{0.5}Na_{0.5})TiO_3 - xBaTiO_3$ (BNT-100$x$BT, $x = 0.0625$ and 0.075) polycrystalline piezoelectric ceramics are investigated using high-energy synchrotron X-ray diffraction. A quantitative comparison between the domain texture results from the full-pattern Rietveld refinement analysis of both single synchrotron diffraction images and full rotation diffraction data is performed. The results show a good agreement between the texture results from different data, demonstrating the validity of quantitative analysis of fiber-type texture based on single high-energy synchrotron diffraction images. The work confirms the applicability of high-energy synchrotron X-diffraction for the *in situ* studies of fiber-type domain texture evolutions in polycrystalline ferroelectrics. It is worth emphasizing that the approach demonstrated here based on a single diffraction image is applicable to the samples with fiber-type orientation distribution; however, it may lead to inaccurate representation of more complicated ODF.

## II. EXPERIMENTS

The lead-free BNT-6.25BT and BNT-7.5BT polycrystalline piezoelectric ceramics were prepared by conventional solid state processing.[15] Bar-shaped samples with dimensions $1.0 \times 1.0 \times 5.0\,mm^3$ suitable for high-energy synchrotron X-ray diffraction measurements were cut from the sintered disks. The electrodes of silver paste were applied on two opposing $1.0 \times 5.0\,mm^2$ surfaces of the bars. Samples were poled at room temperature by applying a complete cycle of bipolar triangular electric field at a maximum strength of 5 kV/mm and a frequency of 25 mHz. High-energy X-ray diffraction experiments were performed on the poled samples after natural aging for approximately 4 h to measure the crystallographic texture in the remanent state at beamline ID15 of the European Synchrotron Radiation Facility. A schematic of the setup is shown in Figure 1. A monochromatic beam of energy 72.72 keV (wavelength 0.17049 Å) and size $200 \times 150\,\mu m^2$ was used. A series of 43 complete Debye–Scherrer diffraction images (scattering angle $2° \le 2\theta \le 10.5°$) were collected in transmission geometry using a Pixium 4700 flat panel area detector[16] with different sample orientations of the poling axis with respect to the incident beam by moving the $\omega$-sample rotation from $-105°$ to 105° in 5° steps. The collected images at each sample orientation were radially integrated into 36 azimuthal sections of width $\Delta\eta = 10°$ using the software package *fit2d*.[17]

Quantitative texture analysis was performed using the Rietveld refinement program MAUD (Materials Analysis Using Diffraction, Version 2.33)[18] following the procedure described by Wenk and Grigull[6] with both single image diffraction data and full rotation diffraction data collected at various sample orientations. The single image data were

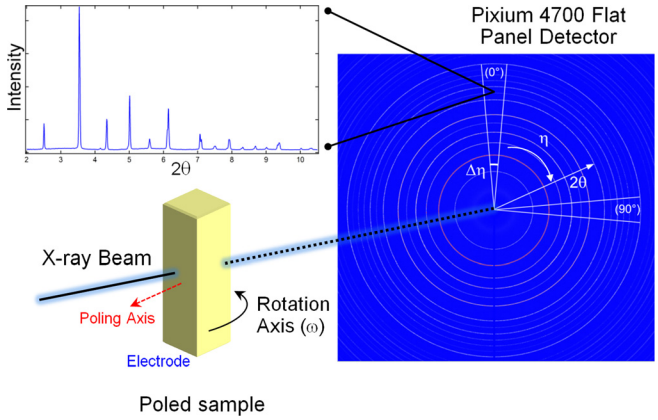


FIG. 1. Schematic diagram of the experimental setup and transmission geometry used for the texture measurement on poled ceramic samples with high-energy synchrotron X-ray diffraction. Note that the shadow areas on the sample represent the silver paste electrodes applied on opposing $1.0 \times 5.0\,mm^2$ surfaces. The red arrow indicates the poling axis of samples that is perpendicular to the electrode plane.

taken with the poling axis perpendicular to the incident beam, as these data represent the diffraction information with the scattering vectors aligned from approximately parallel ($\eta = 90°$) to perpendicular ($\eta = 0°$) to the poling axis, potentially allowing full texture information to be extracted. The structural models of a mixed phase tetragonal-rhombohedral $P4mm + R3c$ for BNT-6.25BT and a single tetragonal phase $P4mm$ for BNT-7.5BT were used in the analysis. The background coefficients, zero offset, lattice parameters, phase fraction, crystal size and microstrain were first refined in MAUD. The absorption correction was then applied prior to the refinement of texture. In the texture refinement with single image data, fiber sample symmetry was enforced, while in the case with full rotation data, no sample symmetry was imposed. The absorption correction was applied in MAUD for all the analyses using an approximate absorption model.[19] The absorption model applies the same description of the sample shape as the harmonic expansion approach developed by Popa[20] for the approximation of general shape of crystallites. In the absorption correction with MAUD, the absorption path of an X-ray beam was calculated from the sample shape, and then the peak intensities were corrected for absorption based on different path lengths through the sample. A weighted strain orientation distribution function (WSODF) model[21] was applied in the refinement to account for the anisotropic lattice strains in the poled samples. The orientation distribution function (ODF) was determined by texture refinements using a fourth-order spherical harmonics model implemented in MAUD. The determined ODF of each phase was exported from MAUD, interpolated on a $5° \times 5° \times 5°$ grid in orientation space and further used to recalculate the complete pole figures using the software package MTEX.[22] To evaluate the difference between the domain textures determined from single image and full rotation data, in addition to the comparison of the features of obtained pole figures such as the pole maxima and minima, the deviation between the two ODFs obtained from different diffraction data is quantified using a normalized square variance sum, as defined by[7]

TABLE I. Results of structure refinements for BNT-7.5BT and BNT-6.25BT materials using single images and full rotation data. Note the lattice parameters and phase fractions (for two-phase BNT-6.25BT) are constrained between the refinements for consistency.

| | | | Fit quality | | | |
|---|---|---|---|---|---|---|
| | | | Single image | | Full rotation data | |
| Structure (fraction) BNT-7.5BT | $a$ (Å) | $c$ (Å) | $R_{wp}$ (%) | $R_p$ (%) | $R_{wp}$ (%) | $R_p$ (%) |
| P4 mm | 3.89300(16) | 3.93450(4) | 11.8 | 6.7 | 8.3 | 6.2 |
| BNT-6.25BT | | | | | | |
| *P4mm* (39.5%) | 3.89004(13) | 3.90588(26) | 13.0 | 7.5 | 8.8 | 5.5 |
| *R3c* (60.5%) | 5.49919(1) | 13.57546(38) | | | | |

$$\varepsilon = \frac{\sum_i \left[f_1(g_i) - f_2(g_i)\right]^2}{\sum_i f_1(g_i)^2}, \quad (1)$$

where $f_1(g_i)$ and $f_2(g_i)$ are the values of the ODFs determined from single image and full rotation data, respectively, and $g_i$ represents the orientation of a crystallite. According to its mathematical definition, the bigger the $\varepsilon$ value, the larger the difference between the two ODFs.

## III. RESULTS AND DISCUSSION

During electrical poling, the volume fraction of ferroelectric domains oriented with their polarization axes *hkl** (e.g., [001] and [111] in the tetragonal and rhombohedral perovskite crystals, respectively) close to the applied electric field direction increases by domain switching. This process results in a remnant domain texture in the case that irreversible domain switching is induced. Unlike the grain texture in engineering materials developed by grain evolution mechanisms, the texture of ferroelectric materials originated from domain switching processes has a unique saturated characteristic, as the reorientation of domains in individual grains is limited to crystallographic symmetry-related directions.[23] Compared with the grain textures in metals having undergone thermo-mechanical processing, the domain texture in the poled ceramics is relatively weak with smooth features.[12,24,25] The full-pattern Rietveld analysis as applied here incorporates a spherical harmonics texture model for the evaluation of domain textures. The Rietveld refinement fits using single image and full rotation data from BNT-7.5BT and BNT-6.25BT materials are shown in Figures S1–S4 in the supplementary material. The analysis yields the complete ODFs for both single-phase ceramics and morphotropic compositions with phase coexistence, allowing the quantification of domain texture distributions. Table I lists the results of the structure models from the Rietveld refinements using single image and full rotation data from two compositions. Figures 2(a) and 2(b) shows the recalculated $002_T$, $200_T$, and $111_T$ pole figures from the ODF for single-phase tetragonal BNT-7.5BT ceramic determined from the texture refinement using single images with the constraint of fiber sample symmetry and full rotation data with no sample symmetry imposed, respectively. In this paper, the pseudocubic indices are used throughout. The subscripts T herein and R in the following refer to the tetragonal and rhombohedral phases, respectively. It is demonstrated in Figs. 2(a) and 2(b) that the pole maxima and minima as quantified in multiples of a random distribution (MRD) are close for corresponding pole figures from the two analyses with a variation in texture magnitudes of ~0.04 MRD. Additionally, as expected in the poled tetragonal BNT-7.5BT material, due to the electric-field-induced non-180° domain switching in the poling

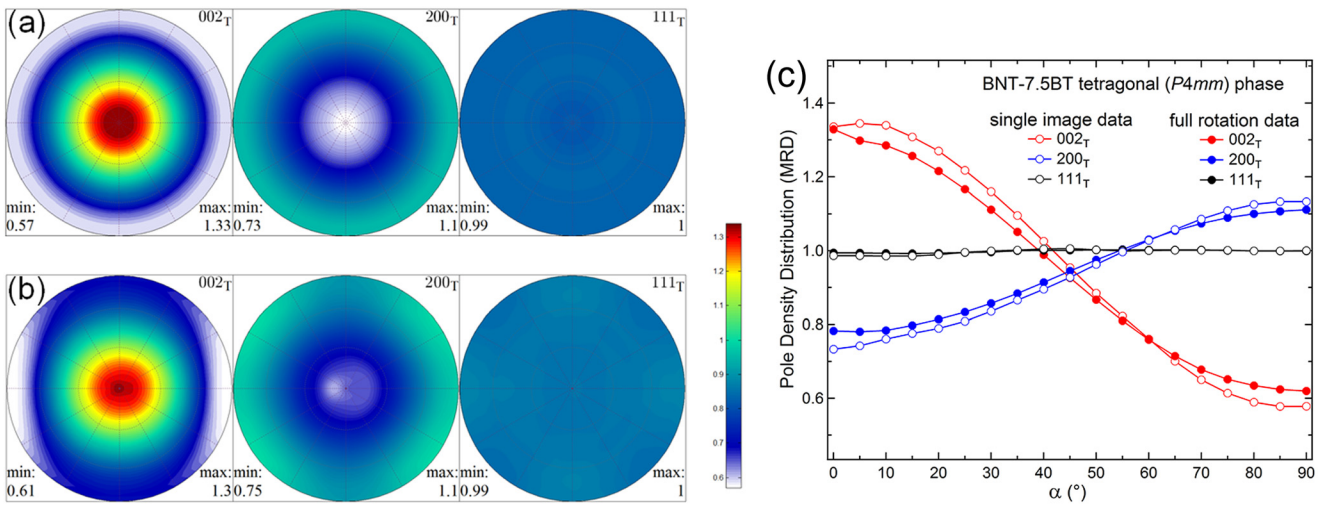


FIG. 2. $002_T$, $200_T$, and $111_T$ pole figures of tetragonal BNT-7.5BT ceramic determined from full-pattern texture refinement using (a) single image data and (b) full rotation data. The data in (c) are extracted from the corresponding pole figures and show the pole density distributions (MRD) at different angles $\alpha$ to the poling axis. The center of the pole figures corresponds to the poling axis (i.e., at $\alpha = 0°$).

TABLE II. Quantitative information for the measured texture of the samples using different data sets.

| Samples | Pole figure maximum (MRD) | ODF maximum (MRD) | Texture index | $\varepsilon$ |
|---|---|---|---|---|
| BNT-7.5BT (single image) | 1.33 | 1.37 | 1.04 | 0.0533 |
| BNT-7.5BT (full rotation) | 1.3 | 1.33 | 1.03 | |
| BNT-6.25BT (tetragonal phase, single image) | 1.58 | 1.6 | 1.04 | 0.1639 |
| BNT-6.25BT (tetragonal phase, full rotation) | 1.55 | 1.58 | 1.05 | |
| BNT-6.25BT (rhombohedral phase, single image) | 2.12 | 2.14 | 1.2 | 0.2108 |
| BNT-6.25BT (rhombohedral phase, full rotation) | 2.15 | 2.18 | 1.2 | |

process, the most pronounced domain texturing effect is observed in the $002_T$ pole figure with the $002_T$ pole maximum in the poling axis (i.e., the center of the pole figures), whereas the $200_T$ pole shows a minimum in the poling axis. In contrast, no $111_T$ domain texture is observed, as indicated by the almost invariant pole densities of ~1 MRD, which is consistent with the fact that the $111_T$ lattice planes are not affected by domain switching in tetragonal ferroelectrics.[26] Furthermore, Figure 2(c) shows the $002_T$, $200_T$, and $111_T$ pole density distributions as a function of the angle $\alpha$ with respect to the poling axis. Some quantitative details of the texture including the pole figure maximum, ODF maximum and texture index are also summarized in Table II. A comparison of the pole profiles (Fig. 2(c)) and the quantitative texture parameters (Table II) confirms that the quantitative texture results for tetragonal BNT-7.5BT extracted from single image and full rotation data are in good agreement. Notably, the difference between the two ODFs from the single image data and full rotation data is small, as indicated by the small error metric value of $\varepsilon = 0.0533$ using Eq. (1). This additional evidence in conjunction with the pole figure results suggests that the actual orientation distribution of domains in poled BNT-7.5BT can be well approximated by the texture derived from the analysis of single image synchrotron X-ray diffraction data without rotating the sample.

The same texture analysis procedures are applied to poled BNT-6.25BT, a material with two co-existing phases

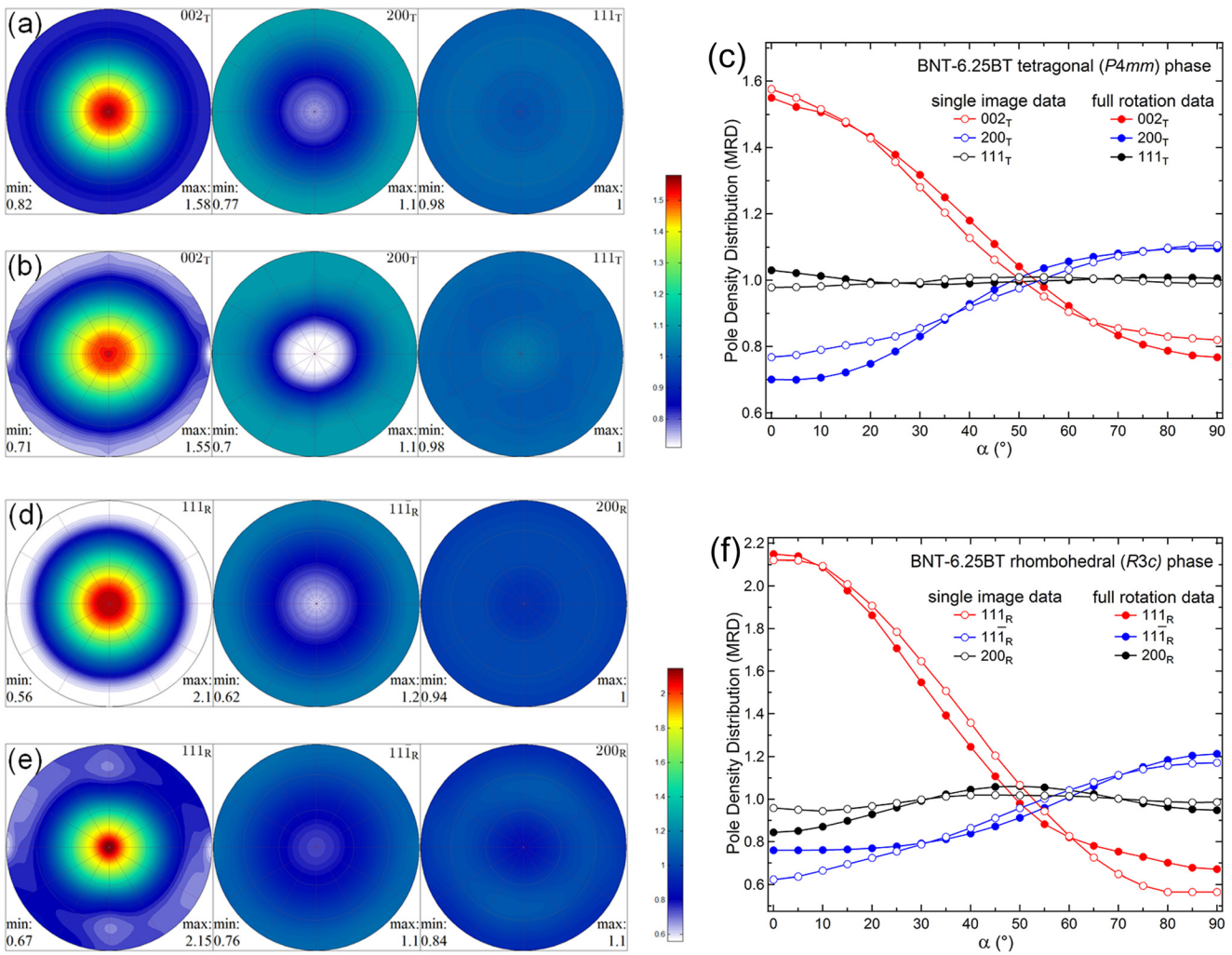


FIG. 3. Pole figures of (a) and (b) tetragonal and (d) and (e) rhombohedral phases for poled BNT-6.25BT ceramic. The pole figures shown in (a) and (d) are obtained from texture refinement using single image data, while those in (b) and (e) are obtained using full rotation data. (c) and (f) The pole density distributions extracted from the corresponding pole figures and represented as a function of the domain orientation angle $\alpha$ to the poling axis.

in the remnant state. Figure 3 displays the recalculated pole figures and corresponding pole profiles of tetragonal and rhombohedral phases in the ceramic derived from both single image and full rotation 2D diffraction data. Consistent with the observation from single-phase BNT-7.5BT, analogous pole figure results are observed for the tetragonal and rhombohedral constitution phases in BNT-6.25BT from the two analyses. The dominant $002_T$ and $111_R$ pole figures observed in poled BNT-6.25BT from the full rotation data (Figs. 3(b) and 3(e)) exhibit a nearly symmetrical distribution of $002_T$ and $111_R$ poles about the sample poling axis (i.e., along the center of pole figures), in good agreement with the observations from single image data (Figs. 3(a) and 3(d)). The pole density and distribution of each phase from the two results (Figs. 3(c) and 3(f)) also show good consistency, with a maximum difference in the pole densities of ~0.15 MRD observed in the dominant $002_T$ and $111_R$ pole profiles. This maximum difference observed in pole density (~0.15 MRD) is approximately 10% of the domain texture strength actually measured. It is noted that the large deviation in the pole density between the single and full rotation image (Figs. 3(c) and 3(f)) is present at $\alpha = 0°$. This is likely related to the fact that the parameters of the spherical harmonic function that represent the ODF are constrained differently in each case. Errors in the analysis can arise from difficulties in the absorption correction during the sample rotation, and this is likely contributing to the observed differences. Additionally, in the single image data, information at exactly $\alpha = 0°$ are not available as the scattering vectors of the measured reflections deviate slightly from the poling axis. Despite these deviations, the pole figure results in Fig. 3 from the two analyses show fairly good agreement, with all the texture features being consistently present, such as the dominant $002_T$ and $111_R$ fiber textures, the preferred $11\bar{1}_R$ domain orientation perpendicular to the poling axis and a random distribution of $200_R$ domains. This is also supported by the similar quantitative texture parameters for each phase obtained from the different analyses as well as the small ODF difference metrics, as shown in Table II. It is thus reasonable to conclude that, consistent with the observation of single-phase BNT-7.5BT, the texture analysis based on single synchrotron image data assuming a fiber sample symmetry is suitable for the evaluation of domain textures in the two-phase BNT-6.25BT ceramic.

Note that the breaking of fiber symmetry is indeed presented in the recalculated pole figures as shown in Figs. 2(b), 3(b), and 3(e) obtained from the texture refinements based on full rotation data and imposing no sample symmetry. The breaking of fiber sample symmetry as well as the small differences observed in the pole distributions is likely related to the complexity of texture analysis processes based on full rotation data, particularly the absorption correction. For the full rotation data measured from the rectangular-shaped samples, the varying peak intensities as a function of orientation originate from two convoluted effects, i.e., the sample absorption variations as a function of orientation as well as the presence of texture. A proper sample absorption correction is thus crucial for the texture analysis using high-energy synchrotron X-ray diffraction. In the analysis of texture based on the single image data, the absorption correction for the flat plate geometry is more simple, while for a rotating rectangle in the case of the analysis with the full rotation data, this is much more difficult and will be prone to errors from slight sample misalignments. These results suggest that in the case of a fiber sample symmetry and a diffraction geometry that requires a complex absorption correction, single image data may counter-intuitively provide a more reliable measure of texture magnitude than full rotation data.

## IV. CONCLUSIONS

In summary, the remanent domain textures in two selected ferroelectric ceramics of BNT-7.5BT and BNT-6.25BT were evaluated by high-energy synchrotron X-ray diffraction. Quantitative texture analysis based on the Rietveld refinement method incorporating spherical harmonics texture models were performed using both single diffraction images and full rotation diffraction data collected with the samples rotated perpendicular to the poling axis. The results of complete pole figures obtained from full rotation data without imposing sample symmetry verify the presence of fiber domain textures in the poled ceramics. A quantitatively good approximation was also observed between the two texture results from the single images and full rotation diffraction data. This work demonstrates that, with a key assumption that the sample has a fiber orientation distribution, the texture analysis using a single high-energy synchrotron diffraction image is suitable for the quantitative evaluation of domain textures in ferroelectric ceramics, validating the reasonable application of high-energy synchrotron X-ray diffraction technique for *in situ* studies of the fiber texture development in polycrystalline ferroelectrics under fast or continuous loading conditions with external stimuli of, for example, electrical and mechanical fields. Despite the advantage of speed of data acquisition by using a single diffraction image for the proper analysis of fiber texture in ferroelectric materials, one has to keep in mind that a single diffraction image would probably not be sufficient to allow an accurate extraction of the ODF for more complicated orientation distributions (e.g., arbitrary texture).

## SUPPLEMENTARY MATERIAL

See supplementary material for the Rietveld refinement fits using single diffraction image and full rotation data measured from BNT-7.5BT and BNT-6.25BT materials.

## ACKNOWLEDGMENTS

This project was in part supported through ARC Discovery Project Nos. DP120103968 and DP130100415. The authors acknowledge the provision of X-ray beamtime by the European Synchrotron Radiation Facility.

[1]J. L. Jones, B. J. Iverson, and K. J. Bowman, J. Am. Ceram. Soc. **90**, 2297 (2007).
[2]A. Pramanick, D. Damjanovic, J. E. Daniels, J. C. Nino, and J. L. Jones, J. Am. Ceram. Soc. **94**, 293 (2011).
[3]N. Setter, D. Damjanovic, L. Eng, G. Fox, S. Gevorgian, S. Hong, A. Kingon, H. Kohlstedt, N. Y. Park, G. B. Stephenson, I. Stolitchnov, A. K. Taganstev, D. V. Taylor, T. Yamada, and S. Streiffer, J. Appl. Phys. **100**, 051606 (2006).

[4]H. Simons, J. E. Daniels, A. J. Studer, J. L. Jones, and M. Hoffman, J. Electroceram. **32**, 283 (2014).
[5]K.-D. Liss, A. Bartels, A. Schreyer, and H. Clemens, Textures Microstruct. **35**, 219 (2003).
[6]H.-R. Wenk and S. Grigull, J. Appl. Crystallogr. **36**, 1040 (2003).
[7]M. Y. Xie, N. Baimpas, C. Reinhard, and A. M. Korsunsky, J. Appl. Phys. **114**, 163502 (2013).
[8]J. E. Daniels, C. Cozzan, S. Ukritnukun, G. Tutuncu, J. Andrieux, J. Glaum, C. Dosch, W. Jo, and J. L. Jones, J. Appl. Phys. **115**, 224104 (2014).
[9]L. Wcislak, H. Klein, H. J. Bunge, U. Garbe, T. Tschentscher, and J. R. Schneider, J. Appl. Crystallogr. **35**, 82 (2002).
[10]G. Ischia, H.-R. Wenk, L. Lutterotti, and F. Berberich, J. Appl. Crystallogr. **38**, 377 (2005).
[11]C. M. Fancher, W. Jo, J. Rödel, J. E. Blendell, and K. J. Bowman, J. Am. Ceram. Soc. **97**, 2557 (2014).
[12]M. C. Ehmke, N. H. Khansur, J. E. Daniels, J. E. Blendell, and K. J. Bowman, Acta Mater. **66**, 340 (2014).
[13]N. H. Khansur, M. Hinterstein, Z. Wang, C. Groh, W. Jo, and J. E. Daniels, Appl. Phys. Lett. **107**, 242902 (2015).
[14]C. M. Fancher, J. E. Blendell, and K. J. Bowman, Appl. Phys. Lett. **110**, 062901 (2017).
[15]W. Jo, J. E. Daniels, J. L. Jones, X. Tan, P. A. Thomas, D. Damjanovic, and J. Rödel, J. Appl. Phys. **109**, 014110 (2011).
[16]J. E. Daniels and M. Drakopoulos, J. Synchrotron Radiat. **16**, 463 (2009).
[17]A. P. Hammersley, S. O. Svensson, M. Hanfland, A. N. Fitch, and D. Hausermann, High Pressure Res. **14**, 235 (1996).
[18]S. Matthies, L. Lutteroti, and H. R. Wenk, J. Appl. Crystallogr. **30**, 31 (1997).
[19]Y. Xie, L. Lutterotti, H. R. Wenk, and F. Kovacs, J. Mater. Sci. **39**, 3329 (2004).
[20]N. Popa, J. Appl. Crystallogr. **31**, 176 (1998).
[21]N. C. Popa and D. Balzar, J. Appl. Crystallogr. **34**, 187 (2001).
[22]R. Hielscher and H. Schaeben, J. Appl. Crystallogr. **41**, 1024 (2008).
[23]J. L. Jones, M. Hoffman, and K. J. Bowman, J. Appl. Phys. **98**, 024115 (2005).
[24]Z. Wang, U. Garbe, H. Li, Y. Wang, A. J. Studer, G. Sun, R. P. Harrison, X. Liao, M. A. V. Alvarez, J. R. Santisteban, and C. Kong, J. Appl. Crystallogr. **47**, 303 (2014).
[25]J. E. Daniels, W. Jo, J. Rodel, and J. L. Jones, Appl. Phys. Lett. **95**, 032904 (2009).
[26]G. Tutuncu, M. Motahari, J. Bernier, M. Varlioglu, J. L. Jones, and E. Ustundag, J. Am. Ceram. Soc. **95**, 3947 (2012).